Journal of Ecology

British Ecological Society

Journal of Ecology 2016, **104**, 1682–1695 doi: 10.1111/1365-2745.12634

Evidence of small-scale spatial structuring of phytoplankton alpha- and beta-diversity in the open ocean

Erik Askov Mousing[1]*, Katherine Richardson[1], Jørgen Bendtsen[2], Ivona Cetinić[3,4] and Mary Jane Perry[5]

[1]Center for Macroecology, Evolution and Climate, Natural History Museum of Denmark, University of Copenhagen, Universitetsparken 15, DK-2100 Copenhagen, Denmark; [2]ClimateLab, Symbion Science Park, Copenhagen, Denmark; [3]NASA Goddard Space Flight Center, Greenbelt, MD, USA; [4]GESTAR/Universities Space Research Association, Columbia, MD, USA; and [5]Darling Marine Center, School of Marine Sciences, University of Maine, Walpole, ME, USA

Summary

1. Phytoplankton assemblages in the open ocean are usually assumed to be mixed on local scales unless large semi-permanent density discontinuities separating water masses are present. Recent modelling studies have, however, suggested that ephemeral submesoscale oceanographic features leading to only subtle density discontinuities may be important for controlling phytoplankton alpha- and beta-diversity patterns. Until now, no empirical evidence has been presented to support this hypothesis.

2. Using hydrographic and taxonomic composition data collected near Iceland during the period of the 2008 spring bloom, we show that the distribution of phytoplankton alpha- and beta-diversity was related to submesoscale heterogeneity in oceanographic conditions. Distinct phytoplankton communities as well as differences in richness were identified on either side of a front delimiting surface waters of slightly different (~0.03) salinities.

3. Alpha-diversity was significantly higher on the high salinity side of the front compared to the low salinity side. This difference was primarily driven by the presence of several large diatom species in the high salinity region, especially of the genus *Chaetoceros* which dominated the biomass here. By investigating beta-diversity in relation to environmental and spatiotemporal variables, we show that the regional distribution of phytoplankton taxa was influenced by both different environmental conditions on either side of the front and dispersal limitation across the front. Changes in beta-diversity were primarily driven by turnover rather than nestedness and were apparently controlled by different processes in each region.

4. *Synthesis.* This study shows that small-scale and ephemeral density discontinuities created by submesoscale frontal dynamics can play a major role in structuring patterns of phytoplankton diversity. Evidence is presented that they can generate changes in environmental conditions (leading to environmental filtering) and act as physical (dispersal) barriers for phytoplankton transport. The study suggests that dispersal barriers are potentially of much greater importance for phytoplankton diversity at local scales than currently recognized and indicates that drivers of marine phytoplankton diversity are similar to those structuring diversity of land plants.

Key-words: beta-diversity, community composition, determinants of plant community diversity and structure, dispersal, niche, phytoplankton, richness, spatiotemporal heterogeneity, submesoscale fronts

Introduction

Understanding the underlying drivers controlling community assemblages and the distribution of life on Earth is a fundamental research objective in ecology. As plants are critical in introducing energy to food webs, particular focus has been devoted to understanding the factors that control their diversity (Connell 1978; Irigoien, Huisman & Harris 2004; Renner 2004; Kier *et al.* 2005; Kraft *et al.* 2011; Chust *et al.* 2013). Most of this research has been conducted in terrestrial

*Correspondence author. E-mail: eamousing@snm.ku.dk

ecosystems where it has long been acknowledged that both dispersal limitation and local environmental conditions are essential components in explaining the distribution of diversity (Hardy & Sonké 2004; Qian, Ricklefs & White 2005; Normand *et al.* 2011).

In the open ocean, microscopic and free-floating phytoplankton are responsible for the vast majority of primary production. Here, in contrast to terrestrial plants, phytoplankton are readily transported with ocean currents and it, therefore, has historically been assumed that dispersal barriers were of little to no importance. Thus, patterns in phytoplankton diversity were, for a long time, believed to be controlled only by local environmental processes and with the entire ocean as the available species pool (i.e. 'everything is everywhere, but the environment selects'; Baas-Becking 1934). With the advent of molecular methods to examine the genetic diversity of organisms, the paradigm of unrestricted dispersal has been challenged (Grosberg & Cunningham 2001; Martiny *et al.* 2006) and it is now clear that global biogeographic patterns in marine plankton distributions do exist (Foissner 2006; Casteleyn *et al.* 2010; Hanson *et al.* 2012; de Vargas *et al.* 2015).

The emerging consensus is that patterns in phytoplankton diversity, similarly to those of plants in terrestrial ecosystems, are at least in part determined by regionally controlled dispersal processes which, in consort with other local processes, that is environmental filtering, biotic interactions and ecological drift, result in contemporary phytoplankton distribution patterns (Tilman, Kilham & Kilham 1982; Kiørboe 1998; Bracco, Provenzale & Scheuring 2000; Hanson *et al.* 2012; Chust *et al.* 2013; e.g. Lévy *et al.* 2015). Both dispersal processes and environmental conditions are, in turn, influenced by oceanographic processes, including current circulation patterns and mesoscale frontal systems which can function as more or less permanent physical barriers and have been shown to separate waters with different dominant phytoplankton species (Claustre *et al.* 1994; d'Ovidio *et al.* 2010; Clayton *et al.* 2013; Clayton, Nagai & Follows 2014; Lévy *et al.* 2014). At regional to global scales, it is relatively easy to envision an interaction between dispersal processes and environmental filtering leading to spatiotemporal structuring of phytoplankton biomass and diversity (Casteleyn *et al.* 2010; Chust *et al.* 2013). However, on small spatial and temporal scales where the lifetime of oceanographic features can become much closer to that of phytoplankton, our understanding of how these various processes work together to influence and maintain phytoplankton diversity is not well developed.

One mechanism that could potentially influence small-scale structuring of phytoplankton diversity at the local scale is the spatiotemporal heterogeneity resulting from submesoscale eddy-driven stratification of the mixed layer and the formation of small-scale oceanographic fronts. Submesoscale oceanographic processes in the upper open ocean often result in temporary separation of a water mass into regions exhibiting differences in hydrographic conditions (Boccaletti, Ferrari & Fox-Kemper 2007; Fox-Kemper & Ferrari 2008). These new hydrographic conditions can lead to altered nutrient/light availability which can potentially have important implications for phytoplankton diversity and activity, that is can lead to patches of increased productivity and biomass within a relatively small geographic region (Lévy, Mémery & Madec 1998; Taylor & Ferrari 2011; Lévy *et al.* 2012; Mahadevan *et al.* 2012).

Submesoscale density discontinuities (fronts) delineating water masses in the open ocean are usually relatively weak and are, therefore, easily broken down. As a result, these fronts are often ephemeral, having expected lifetimes of only days to weeks (Lévy *et al.* 2012). Nevertheless, density discontinuities between the water masses may influence (reduce or prevent) horizontal water movement and these fronts, therefore, might serve as temporary physical barriers for phytoplankton dispersal (Gildor *et al.* 2009). Due to the extremely fast turnover rate of phytoplankton, it is then theoretically possible for the phytoplankton community composition on either side of these fronts to change significantly in the time between front formation and dissolution.

Modelling studies have suggested that the spatiotemporal heterogeneity resulting from submesoscale frontal dynamics may have implications for diversity at the local scale (alpha-diversity) and regional scale (gamma-diversity), as well as drive spatiotemporal differences in phytoplankton community composition (beta-diversity) (Bracco, Provenzale & Scheuring 2000; Perruche *et al.* 2011; Lévy *et al.* 2015). Nevertheless, at present, we have only a limited understanding of how phytoplankton diversity at the local scale is controlled and, to the best of our knowledge, the implications of submesoscale oceanographic features on phytoplankton diversity in the open ocean have never been tested with taxonomic field data.

During the NAB2008 project (Fennel *et al.* 2011), which followed the development of the 2008 spring bloom in the North Atlantic, Mahadevan *et al.* (2012) showed that submesoscale heterogeneity in water column stratification characteristics resulted in the creation of a localized water patch which experienced a phytoplankton bloom several weeks prior to the onset of the regional scale spring bloom. Optical data suggested a greater dominance of diatoms in the patch as compared to surrounding waters (Cetinić *et al.* 2015). Furthermore, the mechanisms that led to the formation of this patch, that is slumping of the north–south density gradient due to instabilities in the mixed layer, would also result in horizontal structuring of the area through the formation of a submesoscale frontal system (Boccaletti, Ferrari & Fox-Kemper 2007; Mahadevan *et al.* 2012).

Here, we present phytoplankton taxonomic data from the area at the time when this patch was found and document that patterns in phytoplankton alpha- and beta-diversity were spatially structured at the submesoscale according to the position the front. On the basis of these observations, we suggest that the subtle density discontinuities (fronts) that commonly occur at the submesoscale in the open ocean may be more important for establishing and maintaining phytoplankton diversity than previously recognized. Furthermore, we suggest that the importance of these features in structuring phytoplankton diversity can stem both from the new environmental

conditions created in association with front formation and because the fronts can act as physical barriers for phytoplankton dispersion.

Materials and methods

COLLECTION AND PROCESSING OF OCEANOGRAPHIC DATA

Data used in the study were collected during the NAB2008 project (Fennel *et al.* 2011) on-board the R/V Knorr in the North Atlantic (25–28°W and 60.6–61.6°N) between 2 and 21 May 2008 (year day 123–142). Conductivity, temperature and depth (CTD) were measured using a Sea-bird Electronics SBE 911 Plus system. The description of the hydrography of the study region is based on 133 CTD determined profiles.

Water samples for determination of nitrate + nitrite (NO_3 + NO_2) and silicic acid (Si) concentrations were collected with 10-L Niskin bottles mounted on the CTD rosette. Water was tapped into acid-washed LDPE bottles, immediately frozen and stored at −20 °C. Frozen samples were thawed in the dark and vigorously mixed (Gordon *et al.* 1993) before spectrophotometric analysis on a Lachat Quickchem 8000 Flow Injection Analysis System (Lachat 1996, 1999). Quality control was performed on the Lachat output spectra and the nutrient profiles according to the recommendations of the IODE workshop on quality control of chemical oceanographic data (IOC 2010).

Mixed-layer depth was determined by defining a maximum density and temperature range in the mixed layer. We note that these ranges are relatively small compared to other studies where warmer areas have been analysed (de Boyer Montégut *et al.* 2004). Mixed-layer depth was defined as the depth representing a change in vertical density of 0.01 kg m^{-3} and a concomitant change in temperature of 0.03 °C. These criteria were necessary because of the relatively small, but significant, changes in temperature and salinity observed in the surface layer during the study period.

All oceanographic data as well as a description of methods used for quality control can be found under the project name 'NAB 2008' at the Biological and Chemical Oceanographic Data Management Office (BCO-DMO; http://osprey.bcodmo.org/project.cfm?flag=view&id=102&sortby=project.)

SAMPLING AND ENUMERATION OF PHYTOPLANKTON DATA

Thirty samples for phytoplankton identification were collected at 16 stations at one or two depths ('surface' at 5 or 10 m; and 'subsurface' at 30 m; Table S1 in Supporting Information). Samples were preserved with acidified Lugol's solution (approximately 2% final concentration). Phytoplankton taxa were determined to the lowest taxonomic level at which an accurate identification could be made using light microscopy and identified by Orbicon A/S, Aarhus, Denmark. Microscopic enumeration of phytoplankton does not allow for a complete description of phytoplankton richness as species smaller than 5 μm become increasingly hard to identify. Thus, the patterns presented in this study primary describe diversity within the microphytoplankton (20–200 μm) and parts of the nanophytoplankton (2–20 μm). The smallest component of phytoplankton community, the picophytoplankton (< 2 μm), is not considered in this study.

Enumeration and calculation of carbon content followed the protocol used in the Danish National Water and Nature Monitoring Program (Henriksen & Kaas 2004). The protocol is only available in Danish, but it is based on the methods described by Utermöhl (1958) and prescribes that at least 500 cells should be counted in each sample, at least 50 cells should be counted for dominant taxa and that single cells should be counted within colonies (see 'Alpha-diversity' section below for more details). Axial dimensions of a subset of each taxon in each sample were measured and used to calculate the biovolume following standard taxon (group)-specific equations (Edler 1979; Helcom 2014). The biovolume was then converted to carbon equivalents using the group-specific conversions presented by Edler (1979). A taxonomic list is presented in Table S2.

DATA ANALYSIS

All statistical analyses were performed in the free and open-source statistical software R version 3.2.3 (R Core Team 2014). In addition to the core software, used the following packages: 'VEGAN' 2.3-3 (Oksanen *et al.* 2016); 'RESHAPE2' version 1.4.1 (Wickham 2007); 'BETAPART' version 1.3 (Baselga *et al.* 2013); 'PLYR' version 1.8.3 (Wickham 2011); 'ECODIST' version 1.2.9 (Goslee & Urban 2007); 'MGCV' version 1.8-11 (Wood 2003); 'GEOR' version 1.7-5.1 (Ribeiro & Diggle 2015), 'RGEOS' version 1.2-3 (Bivand & Rundel 2016); 'GEOSPHERE' version 1.5-1 (Hijmans 2015); and 'MUMIN' version 1.15.6 (Barton 2016).

HYDROGRAPHY

The regional hydrographic patterns and position of the front were assessed by investigating the vertical and horizontal salinity distributions. Salinity was chosen in favour of density and/or temperature because temperature increased during the sampling period (Fig. S2). As stations were sampled only once during the sampling period, the temperature pattern could reflect the temporal development in the region rather than the existence of distinct water masses (see supplementary material for additional supporting analyses).

Patterns of the vertical salinity distribution were examined for the upper 10–200 m of the water column. This depth interval was chosen based on earlier descriptions of the hydrographic characteristics of mixed-layer eddy-driven patch formation (Fox-Kemper & Ferrari 2008; Mahadevan *et al.* 2012). According to Mahadevan *et al.* (2012), water masses at each side of the submesoscale front should differ slightly but consistently in salinity in the upper water column. In order to assess this general expectation, we first constructed a 190 × 133 depth-cast matrix containing 1 m averages of salinity from which we calculated the Euclidian distances between each entry. We then grouped casts with similar profiles by performing a hierarchical clustering analysis on the dissimilarity matrix using complete distance clustering (Legendre & Legendre 2012 chap. 8). Based on this clustering, we calculated the average depth-salinity profiles for the two primary clusters.

Surface salinity in the entire region was interpolated through ordinary kriging (Dale & Fortin 2014). Input data were station coordinates and mean salinity calculated for the upper 10–30 m at each station. Spatial covariance parameters (range = 0.5, nugget = 0, and sill = 0.0004) were determined visually from an empirical variogram of the semi-variance versus spatial distance (Fig. S5).

BETA-DIVERSITY

Beta-diversity, that is differences in community composition between sites/samples, creates a link between local diversity (alpha-diversity)

and the regional species pool (gamma-diversity) and thus provides a powerful framework for studying diversity patterns at various spatiotemporal scales. Beta-diversity can be calculated using a number of different indices all of which have different properties (Legendre & De Cáceres 2013). In this study, we were interested in investigating changes in community composition in relation to spatial, temporal and environmental gradients and we, therefore, chose a similarity driven approach (Vellend 2001; Baselga 2010), that is an approach where pairwise differences in community composition are calculated between all assemblages (samples).

Pairwise dissimilarities can be calculated in several ways, but some of the most commonly used methods in ecology are the Sørensen, Jaccard and Bray–Curtis dissimilarity indices. Here, we calculate beta-diversity using the Sørensen dissimilarity index (β_{sor}) using eqn 1 (Sørensen 1948; Baselga 2010).

$$\beta_{sor} = \frac{b+c}{2a+b+c}, \qquad \text{eqn 1}$$

where a is the number of taxa common between two samples, b is the number of species found in the first sample but not in the second sample, and c is the number of species found in the second sample but not in the first (Baselga 2010). This index is based on presence–absence data, and the result is a dissimilarity matrix which reflects the pairwise differences in taxonomic composition between all samples. This index allowed us to investigate spatiotemporal patterns in the underlying community composition regardless of inter- and intraregional fluctuations in phytoplankton abundance and/or biomass. The Jaccard index is very similar to the Sørensen index and produces almost exactly the same results when applied to our data (Fig. S9). The Bray–Curtis dissimilarity index differs from the other two indices in that abundance/biomass data can be used in its calculation. Calculating beta-diversity with the Bray–Curtis dissimilarity index on double square-root-transformed biomass data (to account for the large fluctuations) led to results very similar to the Sørensen index for our data (Fig. S10). Given the similarity between the analyses, the Sørensen index was chosen as being the most parsimonious.

Structural patterns in taxonomic composition were investigated by performing a non-metric multidimensional scaling analysis (NMDS) on the beta-diversity dissimilarity matrix (Legendre & Legendre 2012). The result is a two-dimensional representation of the differences in community composition between all samples, that is a map of how communities in all samples relate to each other in term of taxonomic composition. In order to compare these structural differences in taxonomic composition with the overall hydrographic structure, we projected the salinity distribution into the NMDS ordination space using thin plate regression splines (Wood 2003). Communities on either side of the front were, thereafter, *a posteriori* classified according to the projected salinity distribution and the two primary clusters identified from the vertical salinity distribution (cut-off salinity 35.245; Fig. 1).

Patterns in beta-diversity can be caused by both nestedness and turnover, where nestedness occurs when the taxonomic composition at a site is a subset of a richer meta-community and turnover occurs when taxa are being replaced by other taxa on a temporal or spatial gradient (Vellend 2001; Baselga 2010; Anderson *et al.* 2011). In order to summarize the relative influence of these underlying mechanisms on beta-diversity in each region, we calculated the multiple-sites dissimilarity index (β_{SOR}) and partitioned it into nestedness (β_{NES}) and turnover (β_{SIM}) following Baselga (2010). The multiple-sites dissimilarity index gives a measure of overall dissimilarity within each group/region but, as this measure (β_{SOR}) can increase with increasing sample size, it was not suitable for comparing between regions in our study. Instead, overall dissimilarity between regions was analysed by comparing the average distance from individual samples to the centroid of each group in the NMDS ordination space. In order to compare nestedness and turnover between groups,

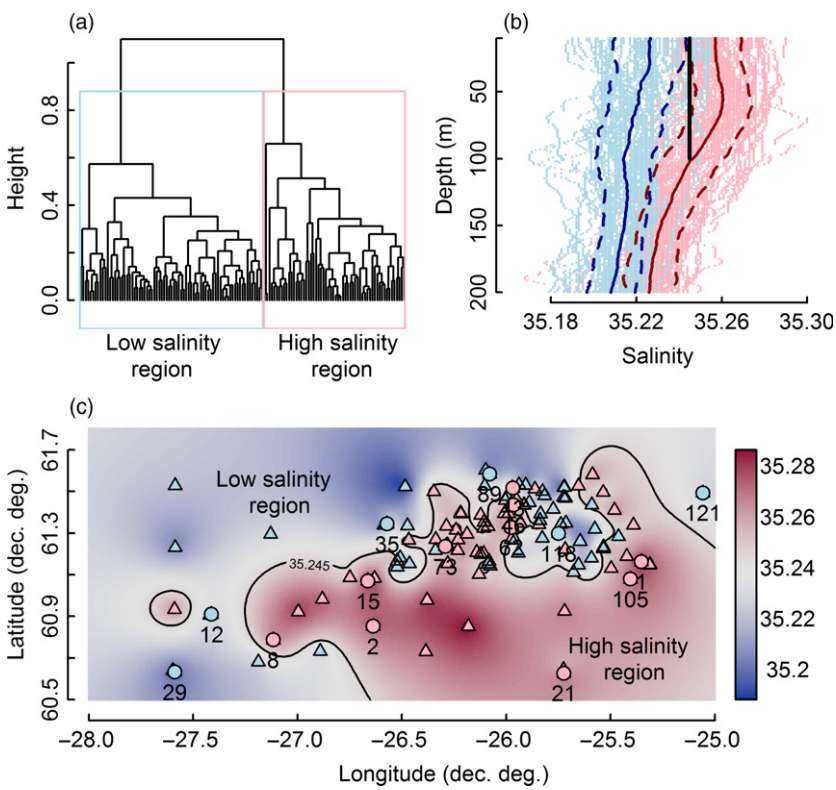

Fig. 1. Vertical and horizontal patterns in salinity: (a) Clustering of the salinity-depth profiles showing the primary regional groups as high salinity (light red) and low salinity (light blue). (b) Average salinity-depth profiles (bold) and standard deviations (dashed) for the two regions. The black line represents salinity = 35.245. (c) Interpolated surface salinity (10–30 m) and position of sampling stations with (circles) and without (triangles) taxonomic information.

β_{NES} and β_{SIM} were standardized as their relative contribution to the multiple-sites dissimilarity index in each region (i.e. β_{NES}/β_{SOR} * 100% and β_{SIM}/β_{SOR} * 100%).

To investigate whether beta-diversity between and within in each region was related to differences in the abiotic variables (i.e. that the taxonomic composition was more similar in samples that resembled each other with respect to space, time, temperature, nutrients, etc.), we calculated the Mantel correlation coefficient (r_m) between beta-diversity (β_{sor}) and the pairwise Euclidian distances between observations of each environmental variable for all samples as well for samples in each region individually. The strength of these correlations was then assessed using Mantel tests with 9999 permutations (Mantel 1967; Legendre & Legendre 2012).

CROSS-FRONTAL BETA-DIVERSITY

To assess the strength of the front as a delimiter of phytoplankton community structure, we performed two analyses. Both analyses are based on the assumption that if there is significant water movement across the front, then we would expect the community composition in samples collected close to the front to be more similar to communities on the opposite side of the front than when samples are collected further away from the front.

In the first analysis, we calculated beta-diversity (β_{sor}) from the subset of pairwise comparisons which crossed the front (i.e. cross-frontal beta-diversity). The relationship between cross-frontal beta-diversity, spatial distance and time was then investigated using multiple linear regression modelling, and the variance explained by each variable was assessed through variance partitioning (Borcard, Legendre & Drapeau 1992; Legendre & Legendre 2012). In the second analysis, we compared the community composition of each sample to the entire community on the opposite side of the front and then related this to the distance to the front. To do this, we first calculated the multiple-sites dissimilarity index (β_{SOR}) for each sample together with all samples on the opposite of the front (i.e. cross-frontal multiple-sites dissimilarity). In order to compare the results from each side of the front, each value was standardized by subtracting mean cross-frontal β_{SOR} calculated for each region. Secondly, based on the horizontal salinity distribution (Fig. 1), we calculated the shortest spatial distance between each sample and the position of the front (i.e. the salinity = 35.245 contour line). The standardized cross-frontal β_{SOR} was then plotted against spatial distance to the front, and the relationship was assessed and tested using the Pearson product–moment correlation coefficient.

ALPHA-DIVERSITY

During the identification process, taxa were determined to different levels, that is, species, genus, family or class (Tables S2 and S3). To determine the alpha-diversity (taxonomic richness) in the two regions, we treated all taxonomic units encountered as being equal. This approach can be justified as it has been shown earlier for other phytoplankton groups (e.g. diatoms: Heino & Soininen 2007) that diversity patterns at the genus and family level reflect patterns at the species level. Thus, while grouping in this manner assumes equal contributions to diversity by all groups (taxonomic levels), we believe it is justified in this study because richness in our data set was strongly correlated across all taxonomic levels (Fig. S6) and because we found no bias in the number of taxa identified at each taxonomic level between regions (Table S3).

Although the enumeration protocol prescribes that at least 500 cells should be counted in each sample, the actual number counted was often much higher because at least 50 (and preferably 100) cells were counted for dominant taxa (Henriksen & Kaas 2004). While this procedure ensures that the abundance and biomass of dominating taxa are quantified to a high degree of precision, it also excludes direct comparison of alpha-diversity between samples and regions. In order to make this comparison, it was necessary to normalize the richness estimates. To do so, we first produced taxon accumulation curves from 1 to 500 by randomly 'drawing' 500 observations based on the relative concentration of each taxon in each sample. We then repeated the process 200 times for each sample and calculated the normalized taxonomic richness as the mean taxonomic richness at 500 draws of the 200 iterations. As the smallest number counted according to the protocol was 500, this procedure is analogous to the technique of rarefaction (Gotelli & Colwell 2001) and the normalized taxonomic richness is, therefore, referred to as 'rarefied'. See Fig. S8 in the supplementary material.

The relationships between taxonomic richness and the measured abiotic variables were investigated using multiple linear regression modelling. The explanatory variables considered were carbon biomass, silicic acid concentrations, nitrate + nitrite concentrations, mixed-layer depth and temperature. In addition, region classification was included as a categorical variable. Data were fitted using ordinary least-squares estimation, and model assumptions of linearity, variance homogeneity and residual normality were checked using visual inspection of the residual patterns. Variable importance was assessed with a model selection approach using AIC_c and the differences in AIC_c between models (ΔAIC_c) (Burnham & Anderson 2003). All possible combinations of explanatory variables were used to model taxonomic richness, and the AIC_c and ΔAIC_c of each model were calculated. The best model (i.e. the best set of explanatory variables) was then identified as the one having the lowest AIC_c.

Results

Clustering of the dissimilarities in the depth-salinity profiles identified two major clusters/groups (Fig. 1a) and the average depth-salinity profiles for these two groups (Fig. 1b) were consistent with the expected 'patch' and 'non-patch' pattern described by Mahadevan *et al.* 2012; that is two water regions separated by front. The salinity differences between the two groups were small (on average 0.032; Table 1) and would not, in themselves, be expected to elicit significant biological responses. The high salinity region identified in our study exhibited a similar overall hydrographic structure as the 'patch' identified by Mahadevan *et al.* (2012) in that there was a pronounced difference in the vertical salinity distribution over the upper 100 m of the water column between the two regions (Fig. 1b). The horizontal salinity distribution showed a relatively narrow transition zone (front) between the two regions. Thus, the front separating the two regions could be roughly defined as occurring at a surface salinity value of 35.245 (Fig. 1b,c).

The high salinity region also exhibited slightly higher temperatures, higher chlorophyll a concentrations and a shallower average mixed-layer depth than the low salinity region on the other side of the front (Table 1) similar to the patterns reported for the area in Mahadevan *et al.* (2012). There were no differences in the average nutrient concentrations

Table 1. Summary statistics of the environmental variables in each region. Values for 'All stations' are based on all measurements in the upper 10–30 m of the water column. Values for 'Tax. stations' are based on the subset of samples where taxonomic information was collected. The *t*-test is performed on all measurements ('All stations')

	High salinity region		Low salinity region				
	All stations Mean (SD)	Tax. stations Mean (SD)	All stations Mean (SD)	Tax. stations Mean (SD)	*t*	d.f.	*P*-value
Salinity	35.257 (0.012)	35.261 (0.018)	35.225 (0.017)	35.220 (0.016)	20.17	251.3	< 0.001
Temperature (°C)	9.21 (0.25)	8.98 (0.36)	8.92 (0.36)	8.83 (0.26)	8.32	250.6	< 0.001
$NO_3 + NO_2$ (μM)	9.55 (1.41)	9.71 (1.63)	9.84 (1.50)	9.75 (0.65)	−1.72	257.1	0.086
Silicic acid (μM)	1.23 (0.99)	1.83 (1.27)	1.27 (0.55)	1.24 (0.35)	−0.48	321.4	0.631
Mixed-layer depth (m)	26.0 (12.0)	29.4 (16.0)	31.0 (13.0)	34.9 (6.2)	−2.25	117.8	0.026
Chlorophyll *a*	2.02 (1.08)	1.91 (1.00)	1.42 (0.66)	1.40 (1.06)	5.70	274.4	< 0.001

(nitrate + nitrite and silicic acid) between the two regions. Nitrate + nitrite were available in concentrations that are usually considered to be non-limiting for phytoplankton growth, whereas silicic acid concentrations were relatively low and possibly limiting for the diatoms in the community. Mean values for the environmental variables examined for the subset of samples that included taxonomic information showed the same patterns as the mean for all stations indicating that the subset of stations where taxonomic information was available was representative of the region in general (Table 1).

The first NMDS ordination axis was strongly correlated to salinity ($r = -0.76$, $P < 0.001$, $n = 30$), indicating that phytoplankton community structure in the study area was strongly associated with changes in salinity (Fig. 2). However, after grouping the samples according to the salinity cut-off value used to define the position of the front (i.e. below or above salinity 35.245), this relationship was absent in both regions ($r = -0.12$, $P = 0.63$, $n = 19$; and $r = -0.50$, $P = 0.11$, $n = 11$). This indicates that the significant 'across-region' relationship with salinity was not driven by a continuous change in community composition with changes in salinity but rather a large change in community composition on either side of the salinity cut-off value. In addition, the salinity-based classification of two phytoplankton communities was supported by hierarchical clustering analysis of the beta-diversity which produced an almost identical grouping pattern (Fig. S7).

In the NMDS ordination space (Fig. 2), the mean distance to the centroid was significantly higher in the low salinity region (0.17 ± 0.07) compared to the high salinity region (0.10 ± 0.05), $t = -2.70$, d.f. = 16.76, $P = 0.015$, indicating that overall region specific beta-diversity (i.e. average difference in community composition between samples) was significantly higher in the low salinity region than in the high. In other words, in addition to being comprised of different

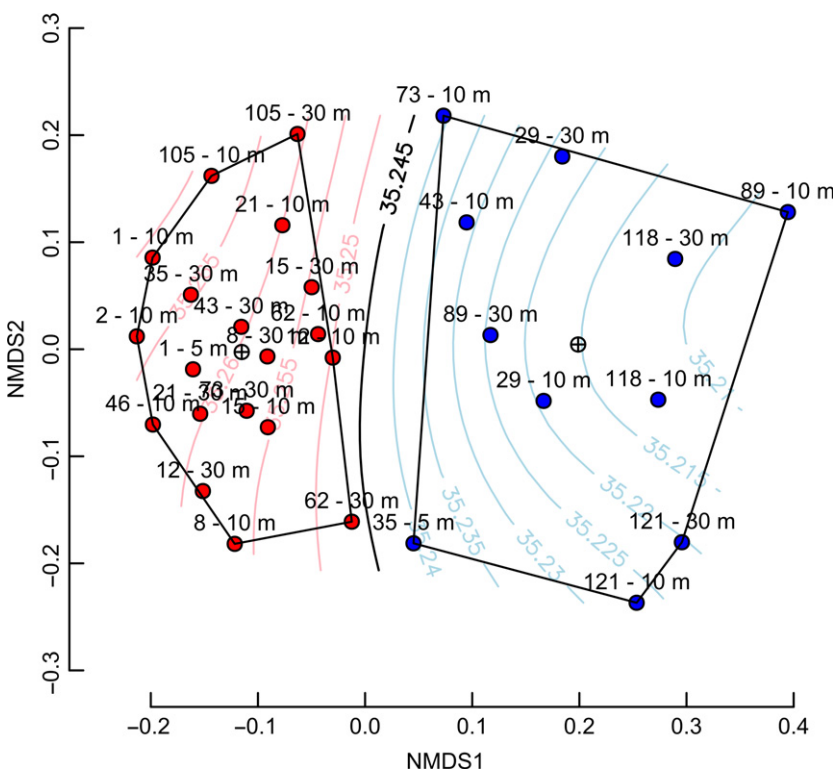

Fig. 2. Non-metric multidimensional scaling (NMDS) ordination plot of beta-diversity. The salinity distribution has been projected into the ordination space as smoothed lines and colour coded according to the salinity-based clustering analysis (Fig. 1) as high salinity (light red) and low salinity (light blue). Samples are grouped as high salinity (red) and low salinity (blue) according to the projected salinity distribution with a cut-off value of salinity = 35.245. The crossed points are the centroids (geometric centres) of the two groups in the ordination space.

phytoplankton communities per se (Figs 2 and 3), the communities in the high and low salinity regions differed in the sense that there was a higher dissimilarity in the community composition between individual samples in the low salinity region than in the higher salinity region.

Partitioning of the multiple-sites dissimilarity (β_{SOR}) into its turnover (β_{SIM}) and nestedness (β_{NES}) components showed a similar pattern in both regions with turnover being the primary driver of change in the community composition (Table 2). The relative contribution of turnover in driving beta-diversity was higher in the high salinity region compared to the low salinity region and increased even more when both regions were considered together (with the opposite being the case for nestedness). It thus appears that changes in community composition between samples both within and between regions are primarily driven by taxonomic replacement.

Across both regions, nine taxonomic groups accounted for more than 85% of the carbon biomass but different groups dominated the biomass in the two regions (Fig. 3). The higher salinity region was dominated by several species of the genus *Chaetoceros* (especially *C. laciniosus*) which, together with *Thalassionema* spp., *Rhizosolenia* spp. and *Pseudo-nitzschia* spp., constituted about 70% of the total carbon biomass. In the lower salinity region, on the other hand, *Cerataulina pelagica*, *Cryptophyceae* spp. and small unidentified flagellates constituted almost 70% of the total carbon biomass. Furthermore, in the higher salinity region, diatoms constituted more than 80% of the total carbon biomass compared to only about 45% in the lower salinity region. However, while the carbon biomasses of dominant taxa were significantly different between regions, there was overlap in the occurrence among the rare taxa where a large proportion of the taxa found in the low salinity region were also found in the high salinity region (Table S2).

Total rarefied taxonomic richness was higher in the high salinity region than in the low (Fig. 4). Taxonomic richness in both regions was positively correlated with total carbon biomass (Fig. 4a) and the silicic acid concentration (Fig. 4b) and negatively correlated with time (Fig. 4c). The best model for explaining taxonomic richness included carbon biomass and silicic acid ($R^2 = 0.73$; Table 3). There was no statistical justification for allowing the groups in the two regions to have different slopes in their relationships to environmental variables (Table S4) indicating that the relationships (Fig. 4a–c) were likely the same in both regions. Silicic acid concentration was found to be negatively correlated with time (Fig. 4d) indicating an active uptake in the diatom community during the sampling period in both regions.

Correlation patterns between beta-diversity (β_{sor}) and dissimilarities in the environmental parameters showed clear differences between the high and low salinity regions (Fig. 5; Table S5). In the high salinity region, beta-diversity was positively correlated with temporal distance (Fig. 5a) and temperature dissimilarity (Fig. 5b). The temperature increased during the sampling period (Fig. S2) and temporal distance and temperature dissimilarity were, therefore, found to be positively correlated ($r_m = 0.47$; $P = 0.002$). In the lower salinity region, however, beta-diversity was not significantly correlated with temporal distance (Fig. 5c), temperature dissimilarity (Fig. 5d), or any other variable investigated (Table S5).

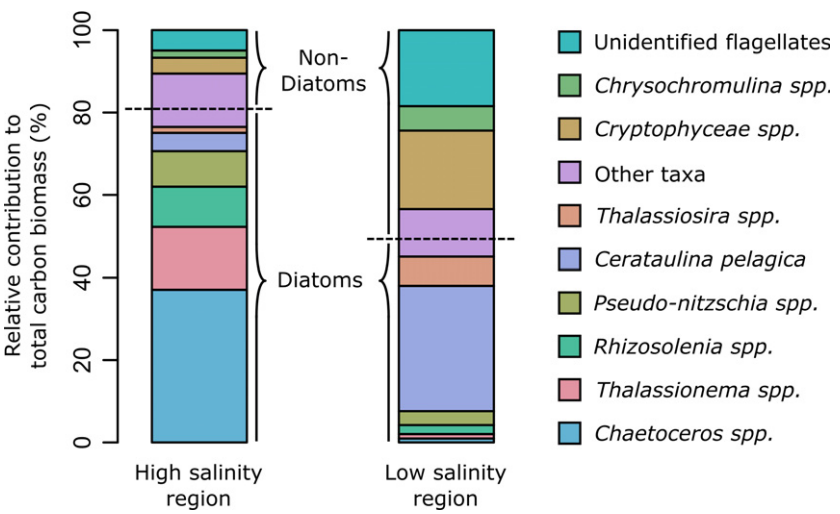

Fig. 3. Relative contribution to total carbon biomass of dominant phytoplankton genera/groups in each region.

Table 2. Absolute and relative differences in multiple-sites dissimilarity, turnover and nestedness for each region

	Multiple-sites dissimilarity (β_{SOR})	Multiple-sites turnover (β_{SIM})	Multiple-sites nestedness (β_{NES})	Turnover relative contribution (β_{SIM}/β_{SOR})	Nestedness relative contribution (β_{NES}/β_{SOR})
High salinity region	0.76	0.68	0.08	89.6%	10.4%
Low salinity region	0.72	0.62	0.10	85.9%	14.1%
Both regions	0.86	0.79	0.07	92.1%	7.9%

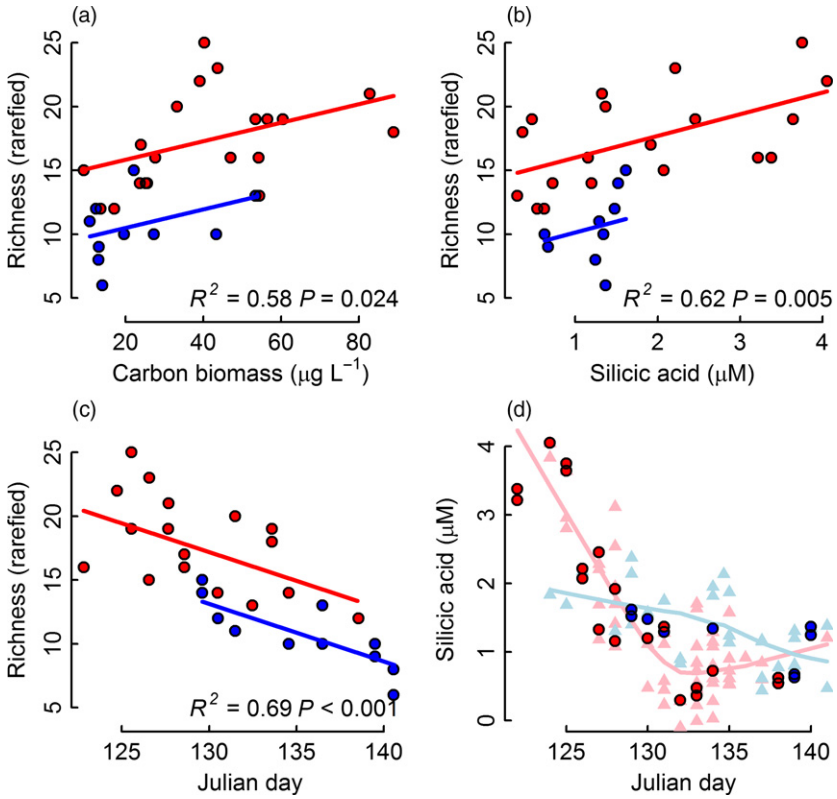

Fig. 4. Bivariate plots of taxonomic richness versus (a) carbon biomass, (b) silicic acid, (c) sampling day and (d) silicic acid versus sampling day, for the high salinity (red) and low salinity (blue) regions. Light red and light blue triangles represent data from stations where taxonomic data were not collected. The smoothing line in (d) represents a Lowess polynomial regression of all data points, whereas the straight lines in (a-c) represent the results of multiple linear regression modelling (Table 3).

Table 3. Model selection using AIC$_c$ and delta-AIC$_c$ (ΔAIC$_c$) for identification of the best environmental variables for explaining taxonomic richness

Model	Formula	R^2	$R^2_{adj.}$	AIC$_c$	ΔAIC$_c$
1	Richness versus Carbon biomass** + Si*** + Region**	0.73	0.70	141.6	0
2	Richness versus Carbon biomass** + Si* + Temp + Region**	0.75	0.71	142.7	1.1
3	Richness versus Carbon biomass** + Si** + NO_3 + NO_2 + Region*	0.73	0.68	144.7	3.1
4	Richness versus Carbon biomass** + Si** + Mixed-layer depth + Region*	0.73	0.68	144.8	3.2
5	Richness versus Carbon biomass** + Si* + NO_3 + NO_2 + Temp + Region**	0.75	0.70	145.7	4.1

Only the top five model candidates are shown. Stars represent significant levels: $P < 0.001$***; $P < 0.01$**; $P < 0.05$*. Full model details are presented in the supplementary material (Table S6).

All analyses where community composition was compared across the front showed no relationship with spatial distance (between sampling sites or distance to the front). Model selection using delta-AIC$_c$ showed that the best model for explaining cross-frontal beta-diversity (i.e. differences in community composition between samples from each side of the front) was a model including only time and this model explained about 15% of the variation (Table 4). Adding spatial distance in addition to time did not add significantly to the explanatory power of the model and variance partitioning revealed that in this model, about 13% of the variation was explained by time alone, about 2% was shared between space and time, and 0% was explained by spatial distance alone (Table S11). Furthermore, cross-frontal multiple-sites dissimilarity (i.e. differences in community composition between each sample and the entire community composition on the opposite side of the front) showed no relationship with increasing distance to the front (Fig. 6). Thus, the spatial distance between samples collected in each region as well as between samples and the position of the front did not significantly impact phytoplankton community composition on either side.

Discussion

In this study, we document that patterns in phytoplankton alpha- and beta-diversity in the open ocean can be strongly correlated with submesoscale oceanographic spatial heterogeneity. The observed diversity patterns are consistent with model- and observation-based predictions concerning phytoplankton diversity in relation to small-scale patchiness and submesoscale frontal dynamics (Claustre *et al.* 1994; d'Ovidio *et al.* 2010; Lévy *et al.* 2012, 2015; Clayton, Nagai & Follows 2014). While the diversity patterns we present here might be predicted to occur based on these

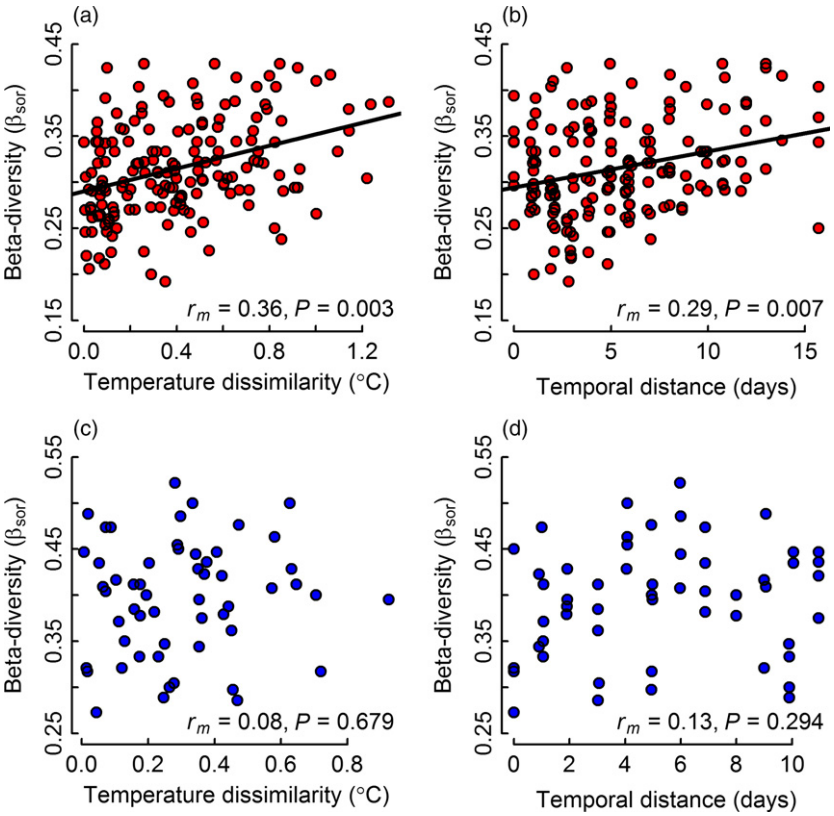

Fig. 5. Bivariate plots of beta-diversity versus (a, c) temperature dissimilarity and (b, d) temporal distance for the (a, b) high salinity and (c, d) low salinity regions.

Table 4. Model selection using AIC_c and delta-AIC_c (ΔAIC_c) for identification of the best spatiotemporal variables for explaining cross-frontal beta-diversity

Model	Formula	R^2	$R^2_{adj.}$	AIC_c	ΔAIC_c
1	Cross-frontal beta-diversity versus Time***	0.15	0.14	−537.3	0
2	Cross-frontal beta-diversity versus Time*** + Spatial distance	0.15	0.14	−535.9	1.35
3	Cross-frontal beta-diversity versus Time* × Spatial distance	0.15	0.14	−534.4	3.03
4	Cross-frontal beta-diversity versus Spatial distance*	0.02	0.01	−508.3	29.00

Stars represent significant levels: $P < 0.001$***; $P < 0.05$*. Variance partitioning of model 2 is presented in the supplementary material (Table S11).

earlier studies, we believe this study is the first that actually demonstrates a relationship between phytoplankton diversity and open ocean small-scale heterogeneity in the physical environment using taxonomic assemblage data rather than bulk measurements of phytoplankton community characteristics.

Phytoplankton community composition was found to be strongly structured in the NMDS ordination space, forming two separate phytoplankton community assemblages delimited by a salinity value of 35.245. This salinity value was also found to horizontally group water masses into two regions with significantly different vertical water column structures. Water properties measured within the two regions were broadly consistent with those expected following the reported formation of a submesoscale front in this region during the time of our study due to eddy-driven slumping of the north–south density gradient (Mahadevan *et al.* 2012); that is significant differences in salinity, temperature, mixed-layer depth and chlorophyll a concentrations were recorded between the two regions (Table 1).

Small-scale spatial structuring of phytoplankton diversity can be explained by either changes in the environment leading to the creation of new niches on each side of the front or the potential of the front to act as a physical barrier limiting dispersal and thus restricting taxa from colonizing the area on the other side of the front. In fact, the presence of a front potentially influences both of these underlying processes. Therefore, patterns generated as a result of environmental differences on both sides of the front and those generated by the front acting as a physical barrier for dispersal will, to a high degree, be spatially correlated.

In both marine and terrestrial ecosystems, environmental conditions play a critical role in determining local taxonomic diversity. We, therefore, assume that one of the primary influences of small-scale oceanographic heterogeneity on the

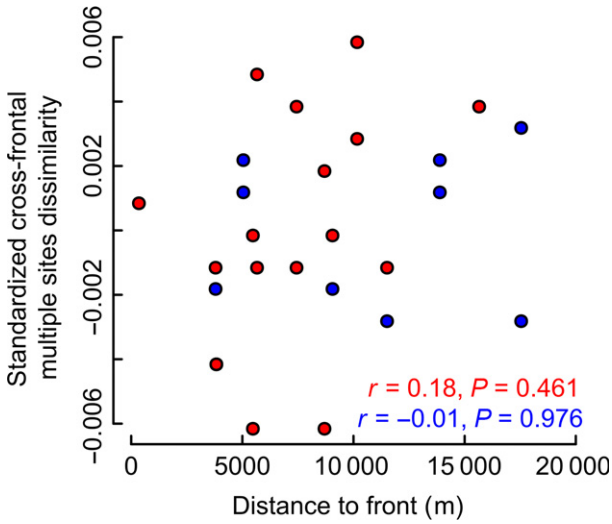

Fig. 6. Standardized cross-frontal multiple-sites dissimilarity plotted against spatial distance to the front in the high salinity region (red) and the low salinity region (blue). Two casts (21 and 29) were sampled farther away than 20 km from the front and are not shown here. All samples were, however, included in the analysis and used to calculate the correlation coefficient.

distribution of phytoplankton diversity operates through localized changes in the availability of limiting resources (e.g. light and nutrients) generated in different oceanographic regimes. Submesoscale front formation and localized stratification lead to changes in the vertical mixing conditions, and these changes potentially impact the nutrients and light available for phytoplankton growth (Fox-Kemper & Ferrari 2008; Johnson, Riser & Karl 2010; Lévy *et al.* 2012). In turn, this would be expected to lead to a change in the phytoplankton community composition (Lévy, Mémery & Madec 1998; Zarauz, Irigoien & Fernandes 2009; Lévy *et al.* 2012; Mahadevan *et al.* 2012).

In the current study, we found significantly different mixing conditions on either side of the front (Table 1). The significantly shallower mixed-layer depths on the side of the front exhibiting higher salinity indicate greater average light availability for surface water phytoplankton on this side of the front. We hypothesize, therefore, that the higher phytoplankton biomass on this side of the front compared to the low salinity side may have been largely due to greater light availability here. While we cannot definitively test this hypothesis, we note that several of the *Chaetoceros* species found almost exclusively in the high salinity side of the front (Table S2) have been reported as being light limited throughout the winter season due to deep mixing but to rapidly increase in abundance and often dominate the phytoplankton biomass (bloom) when light limitation is relieved in the spring (Backhaus *et al.* 2003; Degerlund & Eilertsen 2010).

Sudden environmental changes leading to the creation of new niches and changes in community composition are common in nature (Humborg *et al.* 2000; Hart *et al.* 2005; Barlow & Peres 2008). Although we note that the theory linking disturbances to the maintenance of diversity (i.e. the intermediate-disturbance hypothesis) is controversial and different aspects of disturbance may lead to different diversity responses (Miller, Roxburgh & Shea 2011; Fox 2013), it is clear that the spatial heterogeneity in niche space, which can result from sudden environmental change, can in some cases lead to increases in both beta- and gamma-diversity (Rosenzweig 1995; Ellingsen & Gray 2002; Keith *et al.* 2009). In terms of beta-diversity, our findings are consistent with this situation. Thus, beta-diversity is apparently increased by the disturbance created by the front's formation and changes in mixing conditions on each side (Table 2; Fig. 3).

In terms of gamma-diversity, a large proportion of taxa found in the low salinity region were also encountered in the high salinity region, and the increased spatial heterogeneity found in our study; therefore, only led to a modest increase in total richness in the entire region (i.e. seven taxa which is about a 10% increase; Table S2). However, this apparent similarity between the regions was primarily a result of the collation of taxon lists within regions as the taxonomic composition of individual samples in and between regions showed a high degree of dissimilarity (Table S2). In terms of carbon biomass, however, the two regions exhibited large differences (Fig. 3). Furthermore, similarities between the regions were driven by only a few taxa (e.g. *Nitzschia closterium/longissima* and *Pseudo-nitzschia cf. delicatissima*; Table S2), most of which are small and commonly found generalist taxa in the North Atlantic (Hasle & Syvertsen 1996). Thus, even if richness only showed a small increase following the formation of the front, biodiversity as a whole showed a major increase due to the differences in the distribution of abundance/biomass.

Grazing pressure (top-down control of the phytoplankton community) can also potentially contribute in shaping community composition (Kiørboe 1998). We were not able to measure grazing pressure here but, while we acknowledge that grazing could possibly have modified diversity patterns in both regions, we consider it to be an unlikely candidate for being the primary driver underlying the very large differences detected here between the two regions. If grazing were responsible for the differences noted, then it would have required a selective reduction of *Chaetoceros* spp. and *Thalassionema* spp. to almost undetectable levels in the low salinity region (Fig. 3). In addition, it would require the removal of 20 species in the low salinity compared to the high salinity region and seven species from the high salinity compared to the low salinity region (Table S2).

We were unable in this study to relate the recorded differences in environmental conditions to distribution patterns of individual species. Thus, beta-diversity at the regional scale (both regions together) could not be related to changes in mixed-layer depth or nutrient variability and was instead best described by changes in salinity (Fig. 2; Table S5). When the low and high salinity regions were considered individually, beta-diversity correlated significantly in the high salinity water with temporal distance and temperature dissimilarity (Fig. 5a, b) indicating potential directional community development at all sites and where communities developed from similar primordial communities. In the low salinity region, however, no

relationship between changes in phytoplankton community structure and change in any of the environmental or spatiotemporal variables measured was found.

This apparent lack of relationships between diversity patterns and environmental variables may possibly be explained by a mismatch between the scale at which observations were collected and the scales of the processes that are relevant for regulating phytoplankton diversity (Huston 1999; Whittaker, Willis & Field 2001). Environmental filtering and biotic interactions are local processes (Ricklefs 1987) but, in our study, we seek to infer these processes from samples that are separated in both time and space. So, while we suspect the processes within samples to be more or less the same, the actual pattern in taxonomic composition can be distorted because sample-specific historical processes are erased by the spatial separation.

In summary, we are able to conclude that the observed patterns in the distribution of phytoplankton diversity can to some extent be explained by different local environmental conditions on the two sides of the front. These different environmental conditions are hypothesized to have resulted in different niches developing on each side of the front. Niche and dispersal processes are, however, not mutually exclusive. Even in the case where strong environmental filtering and/or competition/predation pressure would have the effect of quickly reducing the abundance of taxa transported across the front, we would expect to see some evidence of dispersal if it was occurring. Oceanographic fronts restrict water flow regardless of the spatiotemporal scale at which they occur (Gildor *et al.* 2009), and it is, therefore, possible that dispersal limitation across the front could have contributed to the differences in community composition recorded between the two regions.

Larger organisms (e.g. plant seeds, birds and fish) in both terrestrial and aquatic ecosystems disperse as individuals and changes in local diversity therefore take place at the species level; that is single species disperse between areas and will add to local diversity depending on their relative competitive capabilities (Rosenzweig 1995). Phytoplankton, on the other hand, have a very limited capacity for directed movement and horizontal transport over distances of kilometres is only possible through water advection (i.e. they are planktonic). Due to the very large differences in the distribution of the biomass of common species between the regions, traces of cross-frontal dispersal should be relatively easy to identify it occurs. We found, however, no evidence of cross-frontal dispersal.

Cross-frontal beta-diversity, that is, where we compared community similarity between samples on either side of the front, as well as cross-frontal multiple-sites dissimilarity, that is, where we compared community similarity between each sample and the entire community on the opposite side of the front, showed no relationship with increasing distance. Had there been cross-frontal dispersion, we would have expected that phytoplankton communities would have been most similar when the distance between them and/or distance to the front was at a minimum (i.e. a significant distance–decay relationship; Nekola & White 1999; Condit *et al.* 2002). We found, however, no evidence of any community resemblance even among samples that were collected close to each other but where each was on its own side of the front. Furthermore, our analyses showed that cross-frontal beta-diversity increased with time. Hence, the primary factor determining community change at this scale was transitioning across the front, and the dissimilarities between the regions became more pronounced during the sampling period. This strongly indicates that connectivity between the two regions was significantly reduced by the presence of the front.

The data presented here provide ample evidence to conclude that the recorded front served as an effective dispersal barrier during the period of our sampling and that this property can be predicted to have profound implications for the distribution of phytoplankton at larger scales. It has earlier been shown that permanent or semi-permanent mesoscale fronts can effectively delimit differences in both phytoplankton biomass and phytoplankton community composition (Claustre *et al.* 1994; d'Ovidio *et al.* 2010; Clayton, Nagai & Follows 2014). The importance of our study is, therefore, the demonstration that also short-lived and weak fronts created by submesoscale oceanographic processes can have a similar 'barrier effect' with respect to the distribution of phytoplankton alpha- and beta-diversity.

Submesoscale frontal dynamics and localized mixed-layer stratification are coupled to both mesoscale oceanographic features and local weather conditions. Therefore, their importance for the distribution of phytoplankton diversity will probably vary between different regions of the global ocean (Fox-Kemper & Ferrari 2008; Lévy *et al.* 2012). However, satellite-based estimates of the impact of submesoscale stratification on the vertical heat flux have indicated that they may play an important role in large parts of the open ocean including areas with tight atmospheric-ocean coupling (Fox-Kemper & Ferrari 2008).

Thus, there is every reason to believe that the influence of submesoscale frontal dynamics on phytoplankton diversity patterns demonstrated here will be a common feature in the world's oceans. The ubiquitous submesoscale frontal features that are well known from essentially all ocean regions appear to have the potential to create and maintain diversity at the local scale in phytoplankton. These fronts can, apparently, influence diversity both through the creation of different environmental conditions in adjoining water masses and by acting as dispersal barriers for the advective transport of species and communities within relatively small spatial areas. In both terrestrial and marine ecosystems, the importance of local environmental conditions in controlling the distribution of diversity is widely recognized. Dispersal has, however, for a long time been considered to be unrestricted in the ocean, and this has traditionally been considered to be an important difference between the two systems. In this study, we provide empirical evidence that dispersal limitation at small spatial scales can be important in the open ocean and thus, at least in terms of the overall mechanisms controlling diversity, terrestrial and marine systems are not fundamentally different.

Acknowledgements

E.A.M., J.B. and K.R. acknowledge the Danish National Research Foundation for funding the Center for Macroecology, Evolution and Climate (DNRF96). This work was supported by the Danish Research Council for Nature and Universe (KR) and US NSF OCE0628379, OCE0628107 and US NASA NNX08AL92G (MJP).

Data accessibility

Taxonomic data are archived in the Dryad Digital Repository http://dx.doi.org/10.5061/dryad.n0066 (Mousing *et al*. 2016). All oceanographic data as well as a description of methods used for quality control can be found under the project name NAB 2008 at the Biological and Chemical Oceanography Data Management Office (BCO-DMO; http://osprey.bcodmo.org/project.cfm?flag=view&id=102&sortby=project).

References

Anderson, M.J., Crist, T.O., Chase, J.M., Vellend, M., Inouye, B.D., Freestone, A.L. *et al.* (2011) Navigating the multiple meanings of β diversity: a roadmap for the practicing ecologist. *Ecology Letters*, **14**, 19–28.

Baas-Becking, L.G.M. (1934) *Geobiologie; of Inleiding Tot de Milieukunde*. WP Van Stockum & Zoon NV, Den Haag, the Netherlands.

Backhaus, J.O., Hegseth, E.N., Wehde, H., Irigoien, X., Hatten, K. & Logemann, K. (2003) Convection and primary production in winter. *Marine Ecology Progress Series*, **251**, 1–14.

Barlow, J. & Peres, C.A. (2008) Fire-mediated dieback and compositional cascade in an Amazonian forest. *Philosophical Transactions of the Royal Society B, Biological Sciences*, **363**, 1787–1794.

Barton, K. (2016) MuMIn: Multi-Model Inference. https://CRAN.R-project.org/package=MuMIn.

Baselga, A. (2010) Partitioning the turnover and nestedness components of beta diversity. *Global Ecology and Biogeography*, **19**, 134–143.

Baselga, A., Orme, D., Villeger, S., De Bortoli, J. & Leprieur, F. (2013) betapart: Partitioning beta diversity into turnover and nestedness components. URL: http://CRAN.R-project.org/package=betapart.

Bivand, R. & Rundel, C. (2016) rgeos: Interface to Geometry Engine - Open Source (GEOS). https://CRAN.R-project.org/package=rgeos.

Boccaletti, G., Ferrari, R. & Fox-Kemper, B. (2007) Mixed layer instabilities and restratification. *Journal of Physical Oceanography*, **37**, 2228–2250.

Borcard, D., Legendre, P. & Drapeau, P. (1992) Partialling out the spatial component of ecological variation. *Ecology*, **73**, 1045–1055.

de Boyer Montégut, C., Madec, G., Fischer, A.S., Lazar, A. & Iudicone, D. (2004) Mixed layer depth over the global ocean: an examination of profile data and a profile-based climatology. *Journal of Geophysical Research*, **109**, C12003.

Bracco, A., Provenzale, A. & Scheuring, I. (2000) Mesoscale vortices and the paradox of the plankton. *Proceedings of the Royal Society B, Biological Sciences*, **267**, 1795–1800.

Burnham, K.P. & Anderson, D.R. (2003) *Model Selection and Multimodel Inference: A Practical Information-Theoretic Approach*. Springer Verlag, New York, NY, USA.

Casteleyn, G., Leliaert, F., Backeljau, T., Debeer, A.-E., Kotaki, Y., Rhodes, L., Lundholm, N., Sabbe, K. & Vyverman, W. (2010) Limits to gene flow in a cosmopolitan marine planktonic diatom. *Proceedings of the National Academy of Sciences of the United States of America*, **107**, 12952–12957.

Cetinić, I., Perry, M.J., D'Asaro, E., Briggs, N., Poulton, N., Sieracki, M.E. & Lee, C.M. (2015) A simple optical index shows spatial and temporal heterogeneity in phytoplankton community composition during the 2008 North Atlantic Bloom Experiment. *Biogeosciences*, **12**, 2179–2194.

Chust, G., Irigoien, X., Chave, J. & Harris, R.P. (2013) Latitudinal phytoplankton distribution and the neutral theory of biodiversity. *Global Ecology and Biogeography*, **22**, 531–543.

Claustre, H., Kerhervé, P., Marty, J.C., Prieur, L., Videau, C. & Hecq, J.-H. (1994) Phytoplankton dynamics associated with a geostrophic front: ecological and biogeochemical implications. *Journal of Marine Research*, **52**, 711–742.

Clayton, S., Nagai, T. & Follows, M.J. (2014) Fine scale phytoplankton community structure across the Kuroshio Front. *Journal of Plankton Research*, **36**, 1017–1030.

Clayton, S., Dutkiewicz, S., Jahn, O. & Follows, M.J. (2013) Dispersal, eddies, and the diversity of marine phytoplankton. *Limnology and Oceanography, Fluids & Environments*, **3**, 182–197.

Condit, R., Pitman, N., Leigh, E.G. Jr, Chave, J., Terborgh, J., Foster, R.B. *et al.* (2002) Beta-diversity in tropical forest trees. *Science*, **295**, 666–669.

Connell, J.H. (1978) Diversity in tropical rain forests and coral reefs. *Science*, **199**, 1302–1310.

Dale, M.R.T. & Fortin, M.J. (2014) *Spatial Analysis: A Guide for Ecologists*. Cambridge University Press, Cambridge, UK.

Degerlund, M. & Eilertsen, H.C. (2010) Main species characteristics of phytoplankton spring blooms in NE Atlantic and Arctic waters (68–80 N). *Estuaries and Coasts*, **33**, 242–269.

Edler, L. (1979) Recommendations for marine biological studies in the Baltic sea. Phytoplankton and Chlorophyll. *Baltic Marine Biologists Publication 5*, pp. 1–38. Department for Marine Botany, University of Lund, Lund, Sweden.

Ellingsen, K. & Gray, J.S. (2002) Spatial patterns of benthic diversity: is there a latitudinal gradient along the Norwegian continental shelf? *Journal of Animal Ecology*, **71**, 373–389.

Fennel, K., Cetinić, I., D'Asaro, E., Lee, C. & Perry, M.J. (2011) Autonomous data describe North Atlantic spring bloom. *Eos*, **92**, 465–466.

Foissner, W. (2006) Biogeography and dispersal of micro-organisms: a review emphasizing protists. *Acta Protozoologica*, **45**, 111–136.

Fox, J.W. (2013) The intermediate disturbance hypothesis should be abandoned. *Trends in Ecology & Evolution*, **28**, 86–92.

Fox-Kemper, B. & Ferrari, R. (2008) Parameterization of mixed layer eddies. Part II: prognosis and impact. *Journal of Physical Oceanography*, **38**, 1166–1179.

Gildor, H., Fredj, E., Steinbuck, J. & Monismith, S. (2009) Evidence for submesoscale barriers to horizontal mixing in the ocean from current measurements and aerial photographs. *Journal of Physical Oceanography*, **39**, 1975–1983.

Gordon, L.I., Jennings, J.C. Jr, Ross, A.A. & Krest, J.M. (1993) A suggested protocol for continuous flow automated analysis of seawater nutrients (phosphate, nitrate, nitrite and silicic acid) in the WOCE Hydrographic Program and the Joint Global Ocean Fluxes Study. *WOCE Hydrographic Program Office, Methods Manual WHPO 91-1*, pp. 1–55.

Goslee, S. & Urban, D.L. (2007) The ecodist package for dissimilarity-based analysis of ecological data. *Journal of Statistical Software*, **22**, 1–19.

Gotelli, N.J. & Colwell, R.K. (2001) Quantifying biodiversity: procedures and pitfalls in the measurement and comparison of species richness. *Ecology Letters*, **4**, 379–391.

Grosberg, R. & Cunningham, C.W. (2001) Genetic structure in the sea: from populations to communities. *Marine Community Ecology* (eds M.D. Bertness, S. Gaines & M.E. Hay), pp. 61–84. Sinauer Associates, Sunderland, MA, USA.

Hanson, C.A., Fuhrman, J.A., Horner-Devine, M.C. & Martiny, J.B.H. (2012) Beyond biogeographic patterns: processes shaping the microbial landscape. *Nature Reviews: Microbiology*, **10**, 497–506.

Hardy, O.J. & Sonké, B. (2004) Spatial pattern analysis of tree species distribution in a tropical rain forest of Cameroon: assessing the role of limited dispersal and niche differentiation. *Forest Ecology and Management*, **197**, 191–202.

Hart, S.C., DeLuca, T.H., Newman, G.S., MacKenzie, M.D. & Boyle, S.I. (2005) Post-fire vegetative dynamics as drivers of microbial community structure and function in forest soils. *Forest Ecology and Management*, **220**, 166–184.

Hasle, G. & Syvertsen, E. (1996) Marine diatoms. *Identifying Marine Phytoplankton* (ed. R.T. Carmelo), pp. 5–386. Academic Press, New York, NY, USA.

Heino, J. & Soininen, J. (2007) Are higher taxa adequate surrogates for species-level assemblage patterns and species richness in stream organisms? *Biological Conservation*, **137**, 78–89.

Helcom. (2014) Annex C-6 Phytoplankton species composition, abundance and biomass. *Manual for Marine Monitoring in the COMBINE Programme of HELCOM*, pp. C–6 1–21.

Henriksen, P. & Kaas, H. (2004) Fytoplankton artssammensætning, antal, biovolumen og kulstofbiomass. *Tekniske Anvisninger for Marin Overvågning* (eds J. Andersen, S. Markager & G. Ærtebjerg), pp. 1–37. Danmarks Miljøundersøgelser, Miljøministeriet, Danmark.

Hijmans, R.J. (2015) geosphere: Spherical Trigonometry. https://CRAN.R-project.org/package=geosphere.

Humborg, C., Conley, D.J., Rahm, L., Wulff, F., Cociasu, A. & Ittekkot, V. (2000) Silicon retention in river basins: far-reaching effects on biogeochemistry and aquatic food webs in coastal marine environments. *Ambio*, **29**, 45–50.

Huston, M.A. (1999) Local processes and regional patterns: appropriate scales for understanding variation in the diversity of plants and animals. *Oikos*, **86**, 393–401.

IOC (2010) *First IODE Workshop on Quality Control of Chemical Oceanographic Data Collections*. IOC Project for IODE, Oostende, Belgium.

Irigoien, X., Huisman, J. & Harris, R.P. (2004) Global biodiversity patterns of marine phytoplankton and zooplankton. *Nature*, **429**, 863–867.

Johnson, K.S., Riser, S.C. & Karl, D.M. (2010) Nitrate supply from deep to near-surface waters of the North Pacific subtropical gyre. *Nature*, **465**, 1062–1065.

Keith, S.A., Newton, A.C., Morecroft, M.D., Bealey, C.E. & Bullock, J.M. (2009) Taxonomic homogenization of woodland plant communities over 70 years. *Proceedings of the Royal Society B, Biological Sciences*, **276**, 3539–3544.

Kier, G., Mutke, J., Dinerstein, E., Ricketts, T.H., Küper, W., Kreft, H. & Barthlott, W. (2005) Global patterns of plant diversity and floristic knowledge. *Journal of Biogeography*, **32**, 1107–1116.

Kiørboe, T. (1998) Population regulation and role of mesozooplankton in shaping marine pelagic food webs. *Hydrobiologia*, **363**, 13–27.

Kraft, N.J.B., Comita, L.S., Chase, J.M., Sanders, N.J., Swenson, N.G., Crist, T.O. *et al.* (2011) Disentangling the drivers of β diversity along latitudinal and elevational gradients. *Science*, **333**, 1755–1758.

Lachat, I. (1996) Silicate in brackish or seawater–QuickChem Method 31-114-27-1-B. Lachat Instruments, Milwaukee, USA.

Lachat, I. (1999) Nitrate and/or nitrite in brackish or seawater–QuickChem Method 31-107-04-1-A. Lachat Instruments, Milwaukee, WI, USA.

Legendre, P. & De Cáceres, M. (2013) Beta diversity as the variance of community data: dissimilarity coefficients and partitioning. *Ecology Letters*, **16**, 951–963.

Legendre, P. & Legendre, L. (2012) *Numerical Ecology*, 3rd edn. Elsevier, Amsterdam, the Netherlands.

Lévy, M., Mémery, L. & Madec, G. (1998) The onset of a bloom after deep winter convection in the northwestern Mediterranean sea: mesoscale process study with a primitive equation model. *Journal of Marine Systems*, **16**, 7–21.

Lévy, M., Ferrari, R., Franks, P.J.S., Martin, A.P. & Rivière, P. (2012) Bringing physics to life at the submesoscale. *Geophysical Research Letters*, **39**, L14602.

Lévy, M., Jahn, O., Dutkiewicz, S. & Follows, M.J. (2014) Phytoplankton diversity and community structure affected by oceanic dispersal and mesoscale turbulence. *Limnology and Oceanography*, **4**, 67–84.

Lévy, M., Jahn, O., Dutkiewicz, S., Follows, M.J. & d'Ovidio, F. (2015) The dynamical landscape of marine phytoplankton diversity. *Journal of the Royal Society Interface*, **12**, 20150481.

Mahadevan, A., D'Asaro, E., Lee, C. & Perry, M.J. (2012) Eddy-driven stratification initiates North Atlantic spring phytoplankton blooms. *Science*, **337**, 54–58.

Mantel, N. (1967) The detection of disease clustering and a generalized regression approach. *Cancer Research*, **27**, 209–220.

Martiny, J.B.H., Bohannan, B.J.M., Brown, J.H., Colwell, R.K., Fuhrman, J.A., Green, J.L. *et al.* (2006) Microbial biogeography: putting microorganisms on the map. *Nature Reviews: Microbiology*, **4**, 102–112.

Miller, A.D., Roxburgh, S.H. & Shea, K. (2011) How frequency and intensity shape diversity–disturbance relationships. *Proceedings of the National Academy of Sciences of the United States of America*, **108**, 5643–5648.

Mousing, E.A., Richardson, K., Bendtsen, J., Cetiníc, I. & Perry, M.J. (2016) Data from: Evidence of small-scale spatial structuring of phytoplankton alpha- and beta-diversity in the open ocean. *Dryad Digital Repository*, http://dx.doi.org/10.5061/dryad.n0066.

Nekola, J.C. & White, P.S. (1999) The distance decay of similarity in biogeography and ecology. *Journal of Biogeography*, **26**, 867–878.

Normand, S., Ricklefs, R.E., Skov, F., Bladt, J., Tackenberg, O. & Svenning, J.-C. (2011) Postglacial migration supplements climate in determining plant species ranges in Europe. *Proceedings of the Royal Society B, Biological Sciences*, **278**, 3644–3653.

Oksanen, J., Blanchet, F.G., Kindt, R., Legendre, P., Minchin, P.R., O'Hara, R.B., Simpson, G.L., Solymos, P., Stevens, M.H.H. & Wagner, H. (2016) Vegan: Community Ecology Package. URL: http://CRAN.R-project.org/package=vegan.

d'Ovidio, F., De Monte, S., Alvain, S., Dandonneau, Y. & Lévy, M. (2010) Fluid dynamical niches of phytoplankton types. *Proceedings of the National Academy of Sciences of the United States of America*, **107**, 18366–18370.

Perruche, C., Rivière, P., Lapeyre, G., Carton, X. & Pondaven, P. (2011) Effects of surface quasi-geostrophic turbulence on phytoplankton competition and coexistence. *Journal of Marine Research*, **69**, 105–135.

Qian, H., Ricklefs, R.E. & White, P.S. (2005) Beta diversity of angiosperms in temperate floras of eastern Asia and eastern North America. *Ecology Letters*, **8**, 15–22.

R Core Team (2014) *R: A Language and Environment for Statistical Computing*. R Foundation for Statistical Computing, Vienna, Austria. URL: http://www.R-project.org/.

Renner, S. (2004) Plant dispersal across the tropical Atlantic by wind and sea currents. *International Journal of Plant Sciences*, **165**, 23–33.

Ribeiro, P.J. Jr & Diggle, P.J. (2015) geoR: Analysis of Geostatistical Data. https://CRAN.R-project.org/package=geoR

Ricklefs, R.E. (1987) Community diversity: relative roles of local and regional processes. *Science*, **235**, 167–171.

Rosenzweig, M.L. (1995) *Species Diversity in Space and Time*. Cambridge University Press, Cambridge, UK.

Sørensen, T. (1948) A method of establishing groups of equal amplitude in plant sociology based on similarity of species and its application to analyses of the vegetation on Danish commons. *Kongelige Dansk Videnskabers Selskabs Biologiske Skrifter*, **5**, 1–34.

Taylor, J.R. & Ferrari, R. (2011) Ocean fronts trigger high latitude phytoplankton blooms. *Geophysical Research Letters*, **38**, L23601.

Tilman, D., Kilham, S.S. & Kilham, P. (1982) Phytoplankton community ecology: the role of limiting nutrients. *Annual Review of Ecology and Systematics*, **13**, 349–372.

Utermöhl, H. (1958) Zur vervollkommnung der quantitativen phytoplanktonmethodik. *Mitteilungen. Internationale Vereinigung Fuer Theoretische und Angewandte Limnologie*, **9**, 1–38.

de Vargas, C., Audic, S., Henry, N., Decelle, J., Mahe, F., Logares, R. *et al.* (2015) Eukaryotic plankton diversity in the sunlit ocean. *Science*, **348**, 1261605.

Vellend, M. (2001) Do commonly used indices of β-diversity measure species turnover? *Journal of Vegetation Science*, **12**, 545–552.

Whittaker, R.J., Willis, K.J. & Field, R. (2001) Scale and species richness: towards a general, hierarchical theory of species diversity. *Journal of Biogeography*, **28**, 453–470.

Wickham, H. (2007) Reshaping data with the reshape package. *Journal of Statistical Software*, **21**, 1–20.

Wickham, H. (2011) The split-apply-combine strategy for data analysis. *Journal of Statistical Software*, **40**, 1–29.

Wood, S.N. (2003) Thin plate regression splines. *Journal of the Royal Statistical Society. Series B, Statistical Methodology*, **65**, 95–114.

Zarauz, L., Irigoien, X. & Fernandes, J.A. (2009) Changes in plankton size structure and composition, during the generation of a phytoplankton bloom, in the central Cantabrian sea. *Journal of Plankton Research*, **31**, 193–207.

Received 5 February 2016; accepted 27 May 2016
Handling Editor: Will Cornell

Supporting Information

Additional Supporting Information may be found in the online version of this article:

Table S1. Phytoplankton sampling stations (cast numbers), depths and year day of sampling.

Table S2. Taxonomic list with total and percentage number of occurrences in each region. Red and blue highlights represent dominating (based on occurrences) in the high salinity and low salinity regions where taxa were found in more than two-thirds of the samples.

Table S3. Level of identification: the number and percentage of taxa identified at each taxonomic level in each region.

Table S4. Model selection using AIC_c and delta-AIC_c (ΔAIC_c) to assess the evidence of different slopes in the high salinity and low salinity regions of carbon biomass and silicic acid (i.e. interaction between the environmental variables and the patch classification term).

Table S5. Mantel correlation tests of beta-diversity vs. spatiotemporal and environmental variables across all samples and within the high and low salinity regions individually.

Table S6. Full details from the multivariate modeling and selection of the best environmental variables for explaining taxonomic richness. As in the manuscript, only the top five model candidates are shown but all possible combinations were investigated. The 'Region' variable is a factor and the estimate represents the offset in taxonomic richness of the low salinity region in relation to the high salinity region (the intercept).

Table S7a. Full model details relating to the model selection procedure in table S4, i.e. assessment of the evidence of different slopes in the high salinity and low salinity regions of carbon biomass.

Table S7b. Full model details relating to the model selection procedure in table S4, i.e. assessment of the evidence of different slopes in the high salinity and low salinity regions of silicic acid.

Table S8. Results from model comparison of beta-diversity from the entire region (all samples) vs. dissimilarities in salinity and time using AIC_c and delta-AIC_c. Stars represent significant levels: $P < 0.001$***; $P < 0.01$**; $P < 0.05$*.

Table S9. Variance partitioning of the variation in beta-diversity (all samples) that can be explained by salinity and time in a multiple regression model (table S8).

Table S10. Results from model comparison of beta-diversity from the entire region (all samples) vs. dissimilarities in salinity and time using AIC_c and delta-AIC_c. Stars represent significant levels: $P < 0.001$***; $P < 0.01$**; $P < 0.05$*.

Table S11. Variance partitioning of the variation of cross-frontal beta-diversity that can be explained by time and space in a multiple regression model (table 4).

Fig. S1. Horizontal maps of surface temperature (**a**), salinity (**b**) and time-adjusted temperature (**c**; see text). Superimposed on all maps is the contour line where salinity is 35.234 (black lines).

Fig. S2. Temporal air and sea surface changes in the sampling period (**a**). Comparison of temperature changes between the preceding warming period and sea surface temperature offset by four days (**b**). Bivariate plots and Pearson correlation coefficients of the offset sea surface temperature vs. air temperature (**c**).

Fig. S3. Surface temperature (10 m) vs. sampling date for patch (red) and non-patch (blue) stations. The black line represents the fitted values of a generalized additive model.

Fig. S4. Surface salinity (10 m) vs. sampling date.

Fig. S5. Empirical variogram of semi-variance vs. spatial distance.

Fig. S6. Relationship between richness estimates at various taxonomic scales: Upper right half section shows bivariate plots between richness at increasing taxonomic scales (i.e. species, genus, family and class). 'Taxon' represents the grouped scale where all taxonomic units across scales are treated as being equal. Numbers in the lower left panel are Pearson correlation coefficients corresponding to the bi-variate plots in the upper right panel.

Fig. S7. Hierarchical clustering analysis of beta-diversity (β_{sor}) using complete linkage clustering (furthest neighbour sorting).

Fig. S8a,b. Estimation of taxonomic richness: rarefactioning curves for all samples.

Fig. S9. Non-metric multidimensional scaling (NMDS) ordination plot of Jaccard dissimilarity. The salinity distribution has been projected into the ordination space as smoothed lines. Samples are grouped as high salinity (red) and low salinity (blue) according to the projected salinity distribution with a cut-off value of salinity = 35.245. The crossed points are the centroids (geometric centres) of the two groups in the ordination space.

Fig. S10. Non-metric multidimensional scaling (NMDS) ordination plot of Bray-Curtis dissimilarity on double root transformed carbon biomass. The salinity distribution has been projected into the ordination space as smoothed lines. Samples are grouped as high salinity (red) and low salinity (blue) according to the projected salinity distribution with a cut-off value of salinity = 35.245. The crossed points are the centroids (geometric centres) of the two groups in the ordination space.